

Chemo-Genetic Optimization of DNA Recognition by Metallodrugs using a Presenter-Protein Strategy

Jeremy M. Zimbron,^[a] Alessia Sardo,^[a] Tillmann Heinisch,^[a, b] Therese Wohlschlager,^[c] Julieta Gradinaru,^[c] Claudia Massa,^[b] Tilman Schirmer,^{*[b]} Marc Creus,^{*[a]} and Thomas R. Ward^{*[a]}

Dedicated to Dr. R.-Y. Mauverny

Abstract: The mode of action of precious metal anticancer metallodrugs is generally believed to involve DNA as a target. However, the poor specificity of such drugs often requires high doses and leads to undesirable side-effects. With the aim of improving the specificity of a ruthenium piano-stool complex towards DNA, we employed a presenter protein strategy based on the biotin-avidin technology. Guided by the X-ray

structure of the assembly of streptavidin and a biotinylated piano-stool, we explored the formation of metallodrug-mediated ternary complexes with the presenter protein and DNA. The assemblies bound more strongly to telo-

mere G-quadruplexes than to double-stranded DNA; chemo-genetic modifications (varying the complex or mutating the protein) modulated binding to these targets. We suggest that rational targeting of small molecules by presenter proteins could be exploited to bind metallodrugs to preferred macromolecular targets.

Keywords: G-quadruplexes • metallodrug • proteins • ruthenium • supramolecular chemistry

Introduction

DNA is a privileged target of anticancer metallodrugs like cisplatin. However, such drugs often suffer from high toxicity and drug resistance due to non-selective binding to other than oncogenic DNA.^[1] To minimize metallodrug toxicity, several interactions with cancer-associated DNA sequences would be desirable, but such extensive interactions are hard


to achieve with small-molecule drugs. Ultimately, designed assemblies of metallodrugs with presenter proteins^[2] may lead to effective mechanisms of small-molecule delivery to preferred macromolecular targets.

To increase selectivity of small molecule drugs for macromolecular targets, “surface borrowing” can be used to provide additional surface contacts through a presenter protein, which modulates the specificity and affinity of ligand-macromolecule interaction.^[2] The use of bifunctional molecules based on biotin-streptavidin technology has been used for targeting RNA, in which a contribution from protein contacts to the anti-tobramycin RNA aptamer was suggested.^[3] Inspired by these presenter protein strategies and our previous experience of enantioselective artificial metalloenzymes,^[4] we anticipated that metallodrug-mediated protein-DNA interactions could be engineered leading to a stable ternary metallodrug-protein-DNA complex (Figure 1). Such complexes with DNA would be reminiscent of the binding of high-mobility group (HMG)-domain proteins to platinated DNA that mediate cytotoxicity *in vivo*.^[5] Analogous mechanisms of action ultimately involving ternary complexes have also been described for other clinically useful drugs, such as the immunosuppressive antibiotic rapamycin.^[6]

[a] J. M. Zimbron, A. Sardo, T. Heinisch, Dr. M. Creus, Prof. T. R. Ward
University of Basel, Department of Chemistry
Spitalstrasse 51, 4056 Basel (Switzerland)
Fax: (+41) 61 267 1005
E-mail: thomas.ward@unibas.ch
marc.creus@unibas.ch

[b] T. Heinisch, Dr. C. Massa, Prof. T. Schirmer
University of Basel, Biozentrum
Klingelbergstrasse 50/70, 4056 Basel (Switzerland)
Fax: (+41) 61 267 21 09
E-mail: tilman.schirmer@unibas.ch

[c] T. Wohlschlager, Dr. J. Gradinaru
University of Neuchâtel, Institute of Chemistry
Avenue de Bellevaux 51, 2009 Neuchâtel (Switzerland)

 Supporting information for this article is available on the WWW under <http://dx.doi.org/10.1002/chem.201001573>.

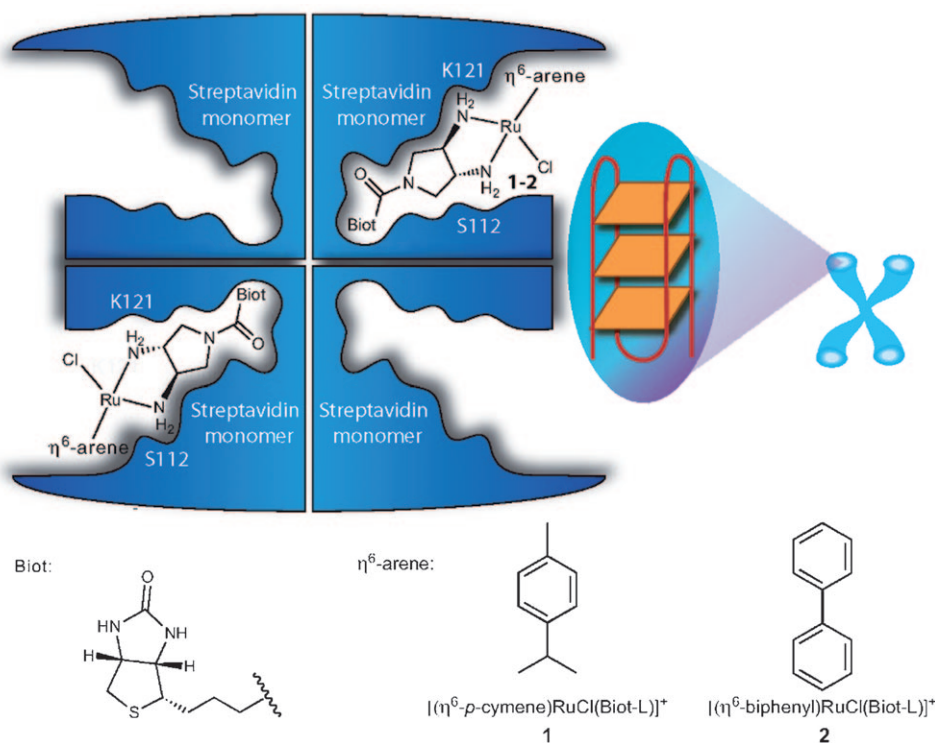


Figure 1. Presenter protein strategy for targeting telomeric DNA with ruthenium metallodrugs. The ruthenium drug embedded into tetrameric Sav in a 2:1 molar ratio forms a supramolecular complex that may allow extensive interactions with a DNA (here depicted as G-quadruplex telomeric DNA; G4A). Chemo-genetic optimization, that is, mutations of defined streptavidin residues (e.g., K121 and S112) or modifying the arene cap of the Ru complex, can modulate the affinity of the assembly for the DNA target. Compound **1** = $[(\eta^6\text{-}p\text{-cymene})\text{Ru}(\text{Biot-L})\text{Cl}]\text{CF}_3\text{SO}_3$ and **2** = $[(\eta^6\text{-biphenyl})\text{Ru}(\text{Biot-L})\text{Cl}]\text{CF}_3\text{SO}_3$; Biot-L = Biotin-*N*-(*R,R*)-3,4-diaminopyrrolidine.

Organometallic drugs have received increasing attention spurred on by their non cross-resistance with Pt-based drugs.^[7] Specifically, the study of ruthenium piano-stool complexes (e.g., see compounds **1** and **2**, Figure 1) as potential anti-tumour drugs has begun to establish structure–activity relationships.^[8] These studies also highlighted the importance of non-covalent interactions in the second coordination-sphere, such as hydrophobic interactions between the η^6 -arene ligand of the piano stool (Figure 1) and DNA that help improve selectivity.^[9] Recently, the nature of the second coordination sphere has also been shown to influence both kinetic- and thermodynamic properties of the binding to proteins, which constitute alternative macromolecular targets of anticancer drugs.^[10]

Results and Discussion

Construction of a presenter protein and metallodrug assembly: As proof-of-concept that target selectivity can be engineered into a supramolecular assembly of drug and presenter protein, we synthesized a biotinylated metallodrug (compound **1**, Figure 1) inspired by promising anticancer Ru^{II} piano-stool complexes,^[7] for incorporation into streptavidin (Sav). The strong binding affinity of Sav for **1** was confirmed

by isothermal titration calorimetry (ITC; $K_d < 60$ nM; Figure 2).

X-ray structure: The crystal structure of the 1C Sav tetramer assembly determined at 2.0 Å resolution (Figure 3 and Supporting Information Figures S1–S3) from protein crystals soaked in excess of **1** shows that the four biotin binding sites are fully occupied by the metallodrug. Ruthenium is coordinated by four ligands, two amino groups of the 3,4-(*R,R*)-ligand, a chloride molecule and the aromatic ring of the *p*-cymene (Table 1). The metal complex has a distorted tetrahedral “piano-stool”-like geometry. In addition to the well documented biotin–Sav interactions,^[11] other interactions between **1** and Sav found in the crystal structure enforce the localisation of the piano-stool moiety within the biotin binding pocket (Figure 3): 1) hydrogen bonding of a diaminopyrrolidine nitrogen to the side

Table 1. Geometrical properties of the primary coordination sphere of the ruthenium in **1** as bound to streptavidin. For simplicity the hydrogen atoms of the amine groups and the neighbouring atoms of the pyrrolidine carbons are omitted. Angles [°] and distances [Å] relative to the *p*-cymene group refer to the centre of the aromatic ring.

$\text{N}^1\text{-Ru-N}^2$	83	$\text{N}^1\text{-Ru}$	2.48
$\text{N}^2\text{-Ru-Cl}$	67	$\text{N}^2\text{-Ru}$	2.37
Cl-Ru-N^1	97	Cl-Ru	2.83
cym-Ru-N^1	130	cym-Ru	1.83
cym-Ru-N^2	139		
cym-Ru-Cl	121		
$\text{N}^1\text{-C}^1\text{-C}^2\text{-N}^1$	89		

chain of S112; 2) apolar interactions of *p*-cymene with Thr114 (Supporting Information, Figure S3) and 3) indirect binding of the labile chloride (or water) ligand to the backbone carbonyl of S122 through a well-ordered water molecule. The diaminopyrrolidine S112 H-bond is reminiscent of a critical interaction between a Pt ligand N–H group and the phosphate backbone of double-stranded DNA (dsDNA)

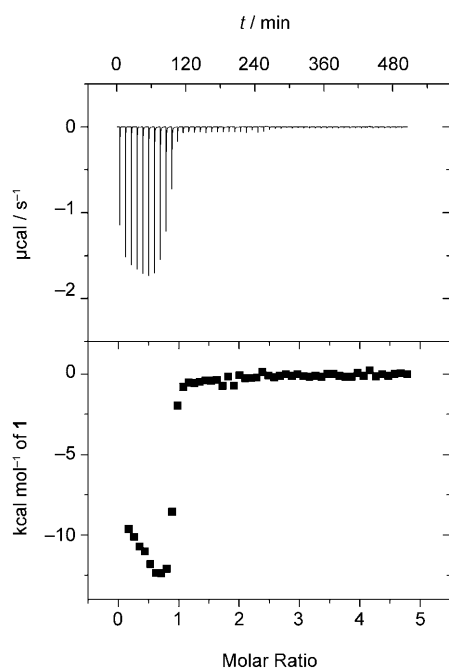


Figure 2. ITC profile for the binding of **1** to Sav. Titration was carried out at 25 °C in 3-(*N*-morpholino)propanesulfonic acid (MOPS) buffer (75 mM) at pH 6.5 with 10 mM of KOH. Every 4 min, 5 μ L of **1** (1 mM) was injected in the reaction cell ($V_{\text{cell}} = 1.5$ mL) filled with Sav (40 μ M of monomer). The heat values are plotted as a function of **1**/Sav molar ratio, to give the corresponding binding isotherms. The resulting isotherms were then fitted to a two set binding sites model. Although binding was strong and probably beyond the sensitivity of ITC, each tetramer of Sav bound approximately four complexes of **1** with affinities of $K_d < 60$ nM.

identified by Lippard in both cisplatin and oxaliplatin X-ray structures.^[12]

In the crystal structure, symmetry related *cis*-Ru atoms are 10.4 Å apart (Figure 3). In the absence of a neighbouring *cis* compound **1** (see Supporting Information: Video 1), the size and charge of the pocket would allow multiple interactions with an incoming DNA molecule. The orientation of the labile Ru–Cl bond is compatible with coordination to electron-rich N⁷ atoms of purines^[13] in an *endo*-base of single-stranded DNA (ssDNA).

Metallo-drug binding to quadruplex DNA: Although the target of DNA-binding metallodrugs is generally thought to be mainly dsDNA, G-quadruplexes also offer attractive alternative therapeutic targets;^[14] they are abundant in telomeres at the end of chromosomes and are found as potential regulatory elements in genes, including oncogenes. Thus, we next investigated the binding of **1**Cav, assembled by mixing two equivalents of complex **1** with one equivalent of tetrameric Sav, to a model G-quadruplex telomeric DNA, namely G4A, consisting of 39 bases (Figures 4 and 5).^[15]

ITC titration (Figure 4a) suggests the formation of a ternary complex between the drug-presenter protein assembly (**1**Cav) and G4A, with sub-micromolar affinity (Table 2,

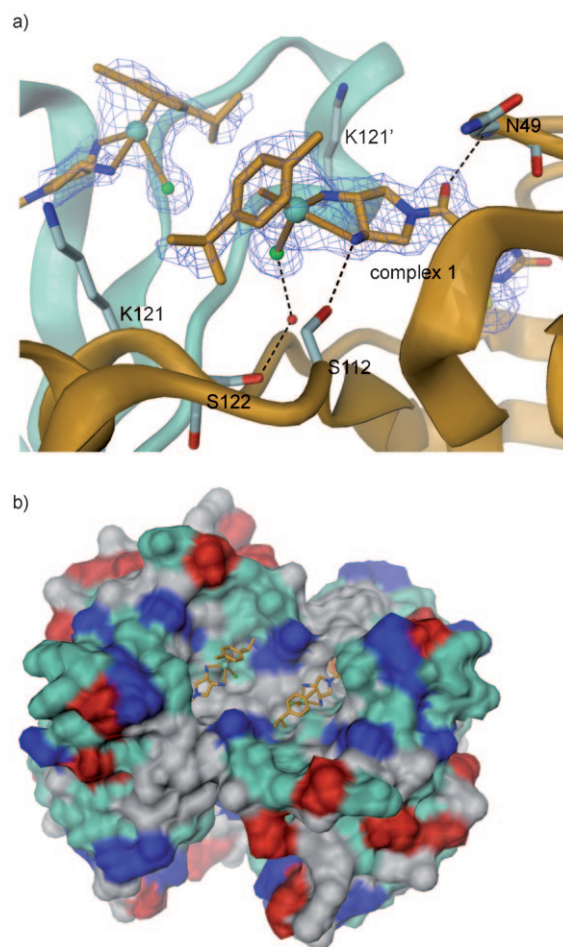


Figure 3. Crystal structure of **1** embedded into the Streptavidin presenter protein (**1**Cav). a) Close-up view of **1** bound to a Sav monomer (orange) also showing the *cis*-related ruthenium moiety (upper-left corner) that is bound to the symmetry-related Sav monomer (aquamarine). Selected Sav residues are shown in full and are labelled. Primed residues belong to the symmetry-related monomer. The 2 Fo–Fc electron density map of **1** is contoured at 1.0 σ . The ruthenium atom is tetrahedrally coordinated by two amino groups of the diaminopyrrolidine, the *p*-cymene and a putative chloride ion (shown in green). b) Molecular surface representation of the Sav tetramer showing two *cis*-related ruthenium moieties. The Sav surface is coloured according to amino acid, with blue = basic residues; red = acidic residues; green = polar residues; grey = hydrophobic residues. The structure has been deposited in the Protein Data Bank (www.pdb.org) with accession code 2WPU.

entry 2). The binding of Sav alone with G4A was markedly weaker in the absence of complex **1** as determined by electrophoretic mobility-shift assays (EMSA; compare Table 2, entries 1 and 2) and by ITC (Figure 4b). EMSA gels (Figure 5) and ITC (Figure 4c) using G4A as target were also carried out with **1** alone (in the absence of Sav). These data reveal the formation of a mixture of fast migrating species that cannot be resolved by EMSA or by ITC, supporting the expected multiple strong binding events to the DNA: there is ample experimental evidence for related Ru piano-stool complexes that display preferential binding to N⁷ guanine in DNA;^[13] a QM–MM calculation predicts a K_d

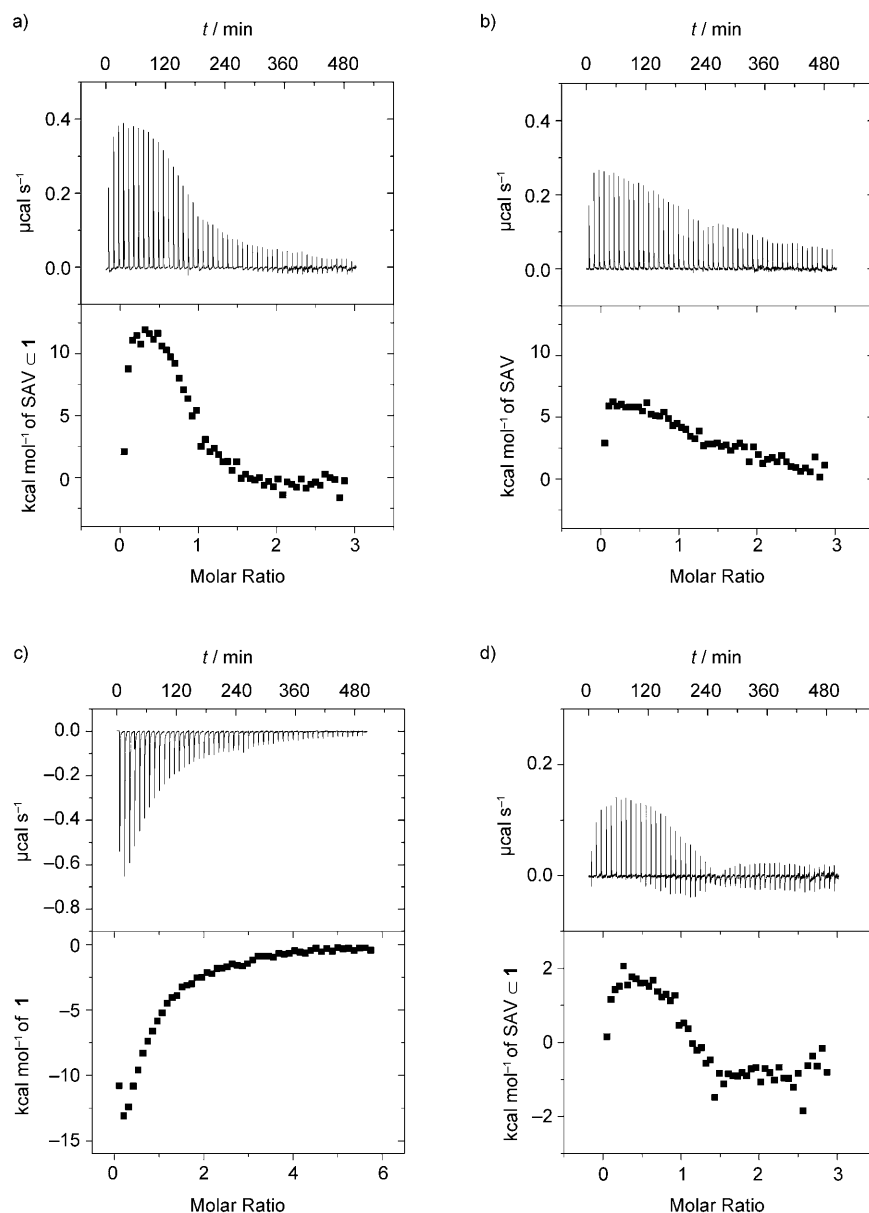


Figure 4. DNA-binding monitored by ITC: a) binding of **1CSav** to G4A: a single set of identical sites model provided an association constant of $(1.35 \pm 0.28) \times 10^6 \text{ M}^{-1}$, enthalpy of $(1.23 \pm 0.355) \times 10^4 \text{ kcal mol}^{-1}$, and stoichiometry of 0.90 ± 0.02 ; b) binding of Sav to G4A: a single set of identical sites model gives an association constant of $(6.56 \pm 2.35) \times 10^4 \text{ M}^{-1}$, enthalpy of $(1.055 \pm 0.124) \times 10^3 \text{ kcal mol}^{-1}$, and stoichiometry of 1.81 ± 0.09 (the binding affinity of the protein alone is more than ten times weaker than in the presence of compound **1**); c) binding of **1** to G4A is apparently strong, exothermic in the conditions used and very different from that found for the ruthenium drug assembled with the presenter protein (see Supporting Information); d) binding of **1CSav** to a “scrambled” telomeric DNA (scG4A) is markedly different and cannot be fitted to a one-site binding-model (compare panels d and a).

of $0.1 \mu\text{M}$ for a related Ru piano stool.^[16] Addition of **1CSav** produced a concentration-dependent change in migration of G4A in EMSA, leading to a single slow migrating species at high concentration that is also consistent with the formation of a ternary complex with a defined 1:1 stoichiometry (DNA/**1CSav**) (Figure 4). Affinities obtained by varying the ratio of **1/Sav** from 1:1 to 4:1 are comparable (Table 2 entries 2, 14 and 15 and Supporting Information Figure S4). The 2:1 ratio was selected for all subsequent studies as it

yielded a well defined 1:1 stoichiometry (**1CSav**/G4A) by ITC (Figure 4a) and EMSA (Figure 5).

Selectivity for single stranded DNA (ssDNA):

To test whether **1CSav** recognizes structural features of G4A or simply its nucleotide content, we used a scrambled telomeric sequence (scG4A) that could not form a G-quadruplex structure. The binding of **1CSav** to this control oligonucleotide (scG4A) was measurably weaker than for G4A, which is bound stoichiometrically in our EMSA assay (Table 2, entries 2 and 11). The ITC titration curve of scG4A could not be fitted to a one-site binding model (Figure 4d). Therefore, under these conditions, **1CSav** binds strongly to the G-quadruplex in a defined 1:1 stoichiometry that fits a single-binding site mechanism and also binds to other ssDNA with marginally less affinity and in a complex mode.

Competitive binding:

To test the selectivity of a ternary complex with DNA in the presence of potentially interfering macromolecules, first competition studies with glutathione were carried out. Glutathione has been shown to coordinate anti-cancer Ru complexes *in vitro*^[17] and has also been implicated in metallodrug inactivation *in vivo*.^[1,18] Although complex **1** could bind glutathione (Supporting Information Figure S5 and Table 2), the presence of a 300-fold excess glutathione with respect to G4A (final concentration of glutathione = 1 mM; i.e., within the physiological range) did not appreciably affect formation of the complex with G4A as evidenced by EMSA (Figure 5).

An excess of competing ssDNA co-incubated with G4A (up to 157 equivalents of competing ssDNA with respect to G4A) lowers binding of the metallodrug-protein assembly as determined by EMSA, but only marginally (Table 2 entries 12 and 13 and Figure 6a). The 12mer ssDNA was better at inhibiting G4A binding than the GGG-trinucleo-

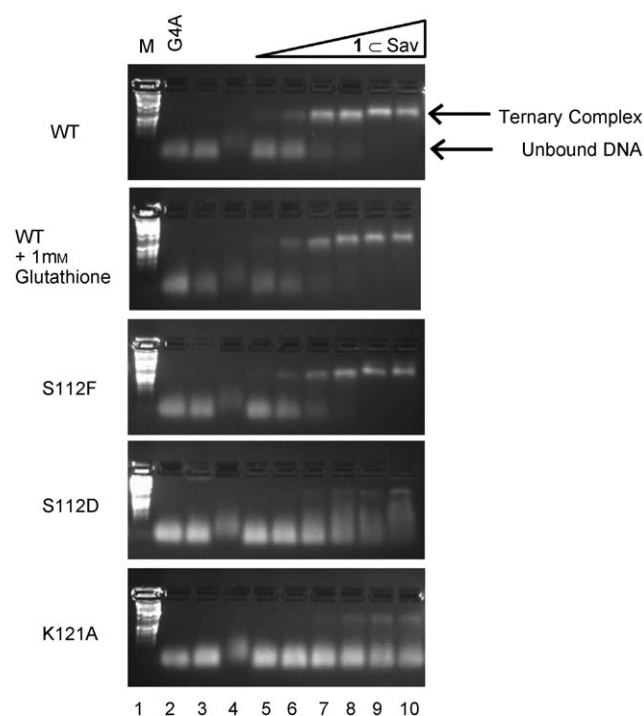


Figure 5. Binding of assembly of metallo-drug and presenter protein (**1CSav**) to G4A monitored by electrophoretic mobility shift assay (EMSA) on agarose gels: EMSA on agarose gels of **1CSav** variants wild-type (WT); WT in the presence of 1 mM glutathione; S112F; S112D or K121A incubated with G4A. Lane 1: DNA Marker. Lane 2: G4A. Lane 3: G4A (3.3 μM) + Sav (39.6 μM); Lane 4: G4A (3.3 μM) + **1** (85.7 μM). Lanes 5–10: G4A (3.3 μM) + **1CSav** at increasing concentrations: 0.8, 1.6, 3.9, 7.9, 19.8, 39.6 μM , representing a **1CSav**/G4A ratio from 0.2 to 12. In all cases 500 ng of DNA was loaded onto the gel.

Table 2. Summary of dissociation constants (K_d) of Ru–Sav assemblies for various DNA targets, as estimated from EMSA.

Entry	DNA Target	Metal complex	Ratio Ru/Sav	Sav	K_d estimated by EMSA [μM]
1	G4A	none	–	WT	>145 ^[a]
2	G4A	1	2	WT	<1.6 ^[b,c]
3	G4A	1	2	S112F	<1.6 ^[c]
4	G4A	1	2	S112D	12.2
5	G4A	1	2	K121A	28
6	G4A	1	2	WT	<1.6 ^[c]
	(GSH) ^[d]				
7	dsOnc	1	2	WT	37.9
8	dsOnc	1	2	S112F	37.9
9	dsOnc	2	2	WT	37.9
10	dsOnc	2	2	S112F	18.2
11	scG4A ^[e]	1	2	WT	2.3
12	G4A	1	2	WT	2
	(GGG) ^[d]				
13	G4A	1	2	WT	5.4
	(12mer) ^[d]				
14	G4A	1	1	WT	2.3
15	G4A	1	4	WT	<1.6 ^[c]

[a] K_d determined by ITC: 15.2 μM (see Supporting Information; Figure S6); [b] K_d determined by ITC: 0.74 μM ; [c] Binding was stoichiometric and probably beyond the sensitivity of these EMSA; [d] In brackets competing species: glutathione (GSH), trinucleotide GGG (GGG) and ssDNA 12mer (12mer); [e] “Scrambled” G4A has identical nucleotide content to G4A but with a different sequence and structure.

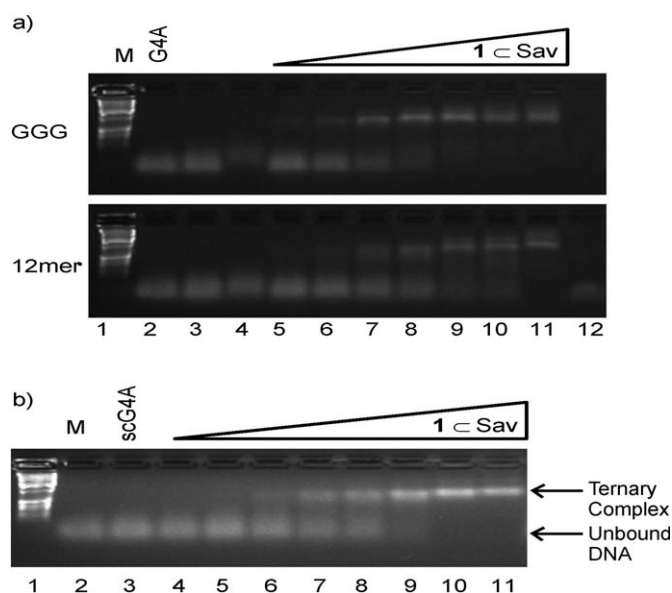


Figure 6. Binding of assembly of metallo-drug and presenter protein (**1CSav**) to ssDNA, monitored by EMSA on agarose-gels: a) Binding to G4A DNA in the presence of competing DNA substrates. Lane 1: Marker (M). Lane 2: G4A. Lane 3: G4A (3 μM) + GGG trinucleotide (206.5 μM) or 12mer ssDNA (462 μM) respectively. Lane 4: G4A (3 μM) + GGG (206.5 μM) or 12mer (462 μM) respectively + complex **1** (76.5 μM). Lane 5–10: GGG (206.5 μM) or 12mer (462 μM) were co-incubated with G4A (3 μM) and the **1CSav** assembly at increasing concentrations: 0.7, 1.4, 3.5, 7, 17.7, 35.3 μM ; under these conditions, the molar ratio **1CSav**/G4A ranges from 0.2 to 12, while GGG/G4A and 12mer/G4A ratio is 69 and 154, respectively. Lane 11: G4A (3 μM) and **1CSav** assembly (35.3 μM). Lane 12: GGG (206.5 μM) or 12mer (462 μM) in the presence of **1CSav** assembly (35.3 μM); GGG or 12mer are barely visible by ethidium bromide staining due to lack of intercalation of the dye in ssDNA. b) Binding to a ssDNA with a “scrambled” G4A sequence (scG4A) unable to form a DNA quadruplex. Lane 1: DNA Marker. Lane 2: ScG4A. Lanes 3–11: G4A (3.3 μM) + **1CSav** at increasing concentrations: 0.4, 0.6, 0.8, 1.6, 3.2, 3.9, 7.9, 19.8, 39.6 μM , representing a **1CSav**/G4A ratio from 0.12 to 12. In all cases 500 ng of scG4A was loaded onto the gel.

tide, which may intimate the existence of a more extended interaction with the **1CSav** assembly compared with the smaller GGG-trinucleotide. These results support the notion that G4A is a privileged target.

Genetic control of the second coordination sphere: Next, we investigated the influence of the second coordination sphere on G4A binding through site-directed mutagenesis. The crystal structure reveals two lysines (K121 of the two adjacent monomers) within 10 Å of the Ru, at the entrance of the largely hydrophobic biotin binding pocket (Figure 3). Mutation of this positively-charged residue (K121A) decreased affinity significantly (Figure 5 and Table 2 entry 5). A decrease in affinity upon lysine mutation has also been observed in other nucleic acid binding proteins^[19] and suggests that the lysines might form a salt bridge with the phosphate backbone. Similarly, the introduction of a negative charge in the vicinity of the Ru (S112D) also reduced binding-affinity (Figure 5 and Table 2 entry 4), perhaps caused

by charge repulsion. In contrast, the introduction of an aromatic residue at the same position (S112F) did not appreciably change the affinity for G4A (Figure 5 and Table 2 entry 3). These results show that DNA binding of the cationic Ru complex **1** is influenced by the second coordination sphere provided by the protein, particularly by charged residues in the vicinity of Ru.

Chemo-genetic optimization for improved binding to dsDNA: We also explored whether Sav could present metallo-drug **1** to dsDNA (Figure 7 and Table 2 entries 7 and 8).

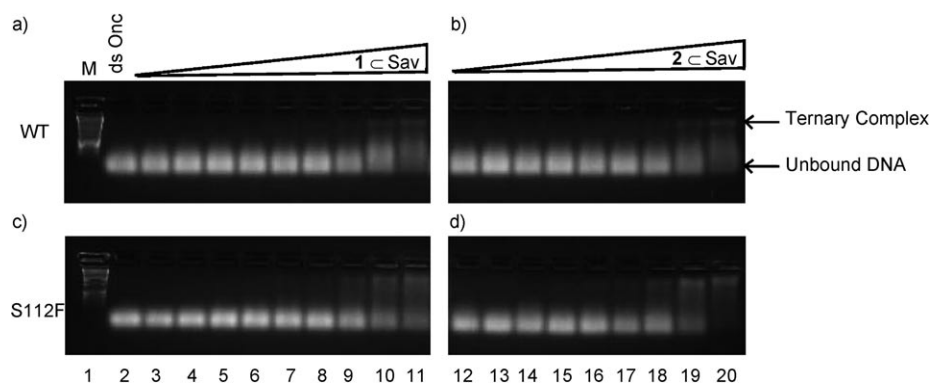


Figure 7. Chemo-genetic optimization of assemblies of drug-presenter proteins improves binding to dsDNA. Comparison of WT streptavidin (a and c) to a genetic variant S112F (b and d) illustrates that the nature of the metallo-drug and presenter protein can influence the binding to dsDNA, as revealed by EMSA on agarose gels. Lane 1: Marker (M). Lane 2: dsOnc. Lanes 3–11: dsOnc (3.12 μM) + concentration increase of **1C**Sav: 0.4, 0.6, 0.8, 1.6, 3.2, 3.9, 7.9, 19.8, 39.6 μM with a **1C**Sav/dsOnc ratio from about 0.12 to 12. Lanes 12–20: dsOnc (3.12 μM) + concentration increase of **2C**Sav: 0.4, 0.6, 0.8, 1.6, 3.2, 3.9, 7.9, 19.8, 39.6 μM with a **2C**Sav/dsOnc ratio from about 0.12 to 12. In all cases 500 ng of DNA was loaded onto the gel.

For this purpose, we used an 18 base pair dsDNA that includes the sequence of the common Braf V599E oncogenic mutation (dsOnc).^[20] Compared with the affinity for G4A ($K_d \approx < 1.6 \mu\text{M}$ as estimated by EMSA; Figure 5), the affinity for dsOnc is significantly lower, with $K_d \approx 37.9 \mu\text{M}$ (Figure 7a and Table 2 entry 7). We hypothesize that a different organization of functional groups, as well as the reduced flexibility of dsDNA, hampers efficient interaction between the ruthenium and nucleophilic sites on the bases. To further demonstrate that DNA binding can be fine-tuned using an assembly of drug and presenter protein, we sought to improve binding to dsDNA chemo-genetically, either with an intercalator,^[21] such as η^6 -biphenyl piano-stool complex **2**, or by genetic introduction of an aromatic residue to the position closest to Ru (S112). The biphenyl-containing S112F variant (**2C**Sav S112F) increased the affinity to dsOnc (Figure 7d and Table 2 entry 10), suggesting that modulation of non-covalent interactions in complexes of metallo-drugs and presenter proteins can be engineered chemo-genetically to afford more specialised binders.

The importance of the extended second coordination sphere that is provided by the presenter protein for selective binding of a small molecule to a macromolecular target is shown by the following: 1) the different modes of binding of

cationic Ru complex **1** to G4A in presence or absence of Sav and 2) the influence of chemogenetic modifications on DNA binding, for example decreasing binding to G4A using a K121A mutant or by increasing the affinity for dsDNA by a judicious combination of genetic variant (S112F) and complex **2** (containing a biphenyl arene cap). In contrast, selective DNA binding is difficult to achieve with small metallo-drugs, such as cationic Ru complex **1** alone, because there are only limited interactions available for recognition of the target.

Conclusion

We have shown that a supra-molecular assembly consisting of a metallo-drug (i.e., biotinylated ruthenium piano stool) combined with a presenter protein (i.e., streptavidin) modulates the recognition profile in vitro through the provision of additional non-covalent interactions. Such extended contacts, which are not typically available to small molecule drugs, allow modulation of affinity and selectivity towards DNA telomeres, even in the presence of competing targets (such as glutathione and dsDNA).

In the present form such assemblies cannot be delivered easily into cells, thus hampering in vivo studies. To overcome this challenge, our current alternative efforts include the following: 1) appending cell-penetrating peptide sequences to the presenter protein; 2) exploring non-DNA,^[10] extracellular targets, which circumvents the need for intracellular delivery and 3) exploiting endogenous species as presenter proteins, such as those overexpressed in cancer cells. The latter would thus only require cell penetration of the metallo-prodrug. The ultimate aim of these experiments is to use such tethered or cross-linking drugs^[6,22] in which an initial kinetic binder^[23] does not merely act as a “carrier”^[24] or “reservoir”^[25] but also chaperones the drug selectively to a macromolecular target in vivo, contributing ultimately to the inhibitory (bio-active) species.

Experimental Section

Experimental details can be found in the Supporting Information.

Acknowledgements

This work was funded by the Swiss National Science Foundation (Grants FN: 200020-113348 and 200020-126366) as well as COST D39 and by generous support to M.C. from the Treubelfonds (Basel). The authors would like to acknowledge Dr. André Ziegler for help with interpretation of ITC data and both Maurus Schmid and Thibaud Rossel for assistance with the design of figures. We are also grateful to C. R. Cantor for the streptavidin expression plasmid and Umicore for a loan of ruthenium.

- [1] L. Kelland, *Nat. Rev. Cancer* **2007**, *7*, 573.
- [2] R. Briesewitz, G. T. Ray, T. J. Wandless, G. R. Crabtree, *Proc. Natl. Acad. Sci. USA* **1999**, *96*, 1953.
- [3] I. Harvey, P. Garneau, J. Pelletier, *Proc. Natl. Acad. Sci. USA* **2002**, *99*, 1882.
- [4] M. Creus, A. Pordea, T. Rossel, A. Sardo, C. Letondor, A. Ivanova, I. Letrong, R. E. Stenkamp, T. R. Ward, *Angew. Chem.* **2008**, *120*, 1422; *Angew. Chem. Int. Ed.* **2008**, *47*, 1400.
- [5] Q. He, U. M. Ohndorf, S. J. Lippard, *Biochemistry* **2000**, *39*, 14426.
- [6] L. A. Banaszynski, C. W. Liu, T. J. Wandless, *J. Am. Chem. Soc.* **2005**, *127*, 4715.
- [7] P. C. Bruijninx, P. J. Sadler, *Curr. Opin. Chem. Biol.* **2008**, *12*, 197.
- [8] a) C. S. Allardyce, P. J. Dyson, D. J. Ellis, S. L. Heath, *Chem. Commun.* **2001**, 1396; b) R. E. Morris, R. E. Aird, P. d. S. Murdoch, H. Chen, J. Cummings, N. D. Hughes, S. Parsons, A. Parkin, G. Boyd, D. I. Jodrell, P. J. Sadler, *J. Med. Chem.* **2001**, *44*, 3616.
- [9] F. Wang, A. Habtemariam, E. P. van der Geer, R. Fernandez, M. Melchart, R. J. Deeth, R. Aird, S. Guichard, F. P. Fabbiani, P. Lozano-Casal, I. D. Oswald, D. I. Jodrell, S. Parsons, P. J. Sadler, *Proc. Natl. Acad. Sci. USA* **2005**, *102*, 18269.
- [10] I. W. McNae, K. Fishburne, A. Habtemariam, T. M. Hunter, M. Melchart, F. Wang, D. M. Walkinshaw, P. J. Sadler, *Chem. Commun.* **2004**, 1786.
- [11] P. C. Weber, D. H. Ohlendorf, J. J. Wendoloski, F. R. Salemme, *Science* **1989**, *243*, 85.
- [12] A. P. Silverman, W. Bu, S. M. Cohen, S. J. Lippard, *J. Biol. Chem.* **2002**, *277*, 49743.
- [13] H.-K. Liu, J. S. Berners-Price, F. Wang, A. J. Parkinson, J. Xu, J. Bella, P. J. Sadler, *Angew. Chem.* **2006**, *118*, 8333; *Angew. Chem. Int. Ed.* **2006**, *45*, 8153.
- [14] S. Balasubramanian, S. Neidle, *Curr. Opin. Chem. Biol.* **2009**, *13*, 345.
- [15] F. X. Han, R. T. Wheelhouse, L. H. Hurley, *J. Am. Chem. Soc.* **1999**, *121*, 3561.
- [16] C. Gossens, I. Tavernelli, U. Rothlisberger, *J. Am. Chem. Soc.* **2008**, *130*, 10921.
- [17] a) C. G. Hartinger, A. Casini, C. Duhot, Y. O. Tsybin, L. Messori, P. J. Dyson, *J. Inorg. Biochem.* **2008**, *102*, 2136; b) F. Wang, S. Weidt, J. Xu, C. L. Mackay, P. R. R. Langridge-Smith, P. J. Sadler, *J. Am. Soc. Mass Spectrom.* **2008**, *19*, 544; c) F. Wang, J. Xu, A. Habtemariam, J. Bella, P. J. Sadler, *J. Am. Chem. Soc.* **2005**, *127*, 17734.
- [18] a) J. Reedijk, *Chem. Rev.* **1999**, *99*, 2499; b) D. Wang, S. J. Lippard, *Nat. Rev. Drug Discovery* **2005**, *4*, 307.
- [19] a) P. Buczek, M. P. Horvath, *J. Mol. Biol.* **2006**, *359*, 1217; b) J. Tan, C. Vonrhein, O. S. Smart, G. Bricogne, M. Bollati, Y. Kusov, G. Hansen, J. R. Mesters, C. L. Schmidt, R. Hilgenfeld, *PLoS Pathog.* **2009**, *5*; c) D. E. Draper, *J. Mol. Biol.* **1999**, *293*, 255.
- [20] H. Namba, M. Nakashima, T. Hayashi, N. Hayashida, S. Maeda, T. I. Rogounovitch, A. Ohtsuru, V. A. Saenko, T. Kanematsu, S. Yamashita, *J. Clin. Endocrinol. Metab.* **2003**, *88*, 4393.
- [21] H. Chen, J. A. Parkinson, S. Parsons, R. A. Coxall, R. O. Gould, P. J. Sadler, *J. Am. Chem. Soc.* **2002**, *124*, 3064.
- [22] a) O. Novakova, A. A. Nazarov, C. G. Hartinger, B. K. Keppler, V. Brabec, *Biochem. Pharmacol.* **2009**, *77*, 364; b) W. H. Ang, A. De Luca, C. Chapuis-Bernasconi, L. Juillerat-Jeanneret, M. Lo Bello, P. J. Dyson, *ChemMedChem* **2007**, *2*, 1799; c) K. R. Barnes, A. Kutikov, S. J. Lippard, *Chem. Biol.* **2004**, *11*, 557; d) G. Jaouen, S. Top, A. Vessières, G. Leclercq, M. J. McGlinchey, *Curr. Med. Chem.* **2004**, *11*, 2505.
- [23] a) A. R. Timerbaev, C. G. Hartinger, S. S. Aleksenko, B. K. Keppler, *Chem. Rev.* **2006**, *106*, 2224; b) A. Casini, C. Gabbiani, E. Michelucci, G. Pieraccini, G. Moneti, P. J. Dyson, L. Messori, *J. Biol. Inorg. Chem.* **2009**, *14*, 761; c) J. Reedijk, *Proc. Natl. Acad. Sci. USA* **2003**, *100*, 3611.
- [24] F. Kratz, *J. Controlled Release* **2008**, *132*, 171.
- [25] B. Wu, P. Droge, C. A. Davey, *Nat. Chem. Biol.* **2008**, *4*, 110.

Received: June 4, 2010
Published online: September 28, 2010